

High Order Sliding Mode Control for Power Regulation: Comparative Insights with PI Controller CUK Converter Implementation

Muhammed Mahho^{ID}^a, Mehmet Yilmaz^{ID}^b and Muhammed Fatih Çorapsız^{ID}^c

Department of Electrical and Electronics Engineering, Ataturk University, Erzurum, Turkey

Keywords: CUK Converter, Proportional-Integral (PI) Controller, High Order Sliding Mode Control (HOSMC), Energy Conversion Efficiency.

Abstract: In this study, the performance analysis of the Higher Order Sliding Mode Controller (HOSMC) and Proportional-Integral (PI) controller for various scenarios was performed using the DC-DC CUK converter topology. While performing the performance analysis, the current ripple at the converter output, voltage rise-fall and convergence time were considered. While comparing the PI controller and HOSMC, the output voltage boost for the 30V input voltage was evaluated to 60V in the first scenario and to 45V in the second scenario. In these scenarios, HOSMC showed superior performance compared to PI controller in a shorter time. In the third scenario, the performance of the controllers was examined to obtain an output voltage lower than the input voltage. In the third scenario, HOSMC provided the desired output voltage at the input voltage level within 0.05s. In this scenario, HOSMC gave more successful results than the PI controller. In the fourth scenario, the input voltage was transferred to the output at different voltage levels at 1.5s intervals. In the fourth scenario, for the first 1.5 seconds, HOSMC has shorter settling time than the PI controller. In the second 1.5 seconds, although the HOSMC experienced some deterioration in the transient state, the desired output voltage values were reached in the same time as the PI controller.

1 INTRODUCTION

Rapid developments in medical devices, computer systems and energy production technologies have increasingly increased the importance of DC-DC converters. Converters are among the basic components that increase energy efficiency by providing different voltage levels required by electronic devices and systems (Yilmaz et al., 2025). Used in a wide variety of applications, from portable devices and electric vehicles to renewable energy systems and communication infrastructures, these converters not only directly contribute to design criteria such as size, weight, and cost, but also improve system performance. The most frequently preferred among switched non-isolated DC-DC converters are; Boost converter, Buck converter, Buck-Boost converter, CUK converter and SEPIC converter. Non-isolated DC-DC converters offer higher efficiency than isolated DC-DC converters and the advantage of voltage increase/decrease via a single switching control. Technological advance-

ments and increasing energy demand have enabled the widespread use of these types of converters. DC-DC converter topologies are frequently used to reduce energy conversion losses in charging systems and PV energy generation systems (Fathabadi, 2016; Mahho et al., 2025). In today's conditions, especially in solar, wind, proton exchange membrane fuel cells and similar energy production systems, the energy produced is low and the current is not constant (Refaat et al., 2024). In such systems, DC-DC converters play a critical role in ensuring that the produced energy is made available for the load systems in a safe and efficient manner (Xu et al., 2021). The CUK converter was proposed by Slobodan Čuk in 1977. This converter is a type of converter that can operate in a step-up/step-down mode without applying a pulse signal to the capacitor in the middle and does not switch from input to output (Ilman et al., 2019). Various control methods, including fuzzy logic (Balestrino et al., 2002) and sliding mode control (Chen, 2012), have been applied to the CUK converter to improve performance criteria such as settling time, steady-state error and overshoot. In (Chen, 2012), two different control methods, Proportional-Integral (PI) con-

^a^{ID} <https://orcid.org/0009-0005-0938-7031>

^b^{ID} <https://orcid.org/0000-0001-7624-4245>

^c^{ID} <https://orcid.org/0000-0001-5692-8367>

trol and Sliding Mode Control (SMC), were used for the CUK converter topology to evaluate the controller performances to obtain constant output voltage. The transient and steady-state performances of the system were analyzed. It was obtained that SMC gave better dynamic response than the PI controller, was superior in terms of stability and was more robust against load changes. In this study, two different methods of voltage control were implemented in the CUK converter topology. These methods are High Order Sliding Mode Control (HOSMC) and PI controller. The two controllers were evaluated for four different scenarios. The scenarios include increasing/decreasing the voltage and changing the voltage levels at certain time intervals.

2 MATERIALS AND METHOD

2.1 DC-DC CUK Converter Topology

Power electronics gained an important role in semiconductor technology in the 1950s with the development of silicon-controlled rectifiers (SCRs), MOSFETs and IGBTs for commercial and industrial applications. Fast switching and reduced losses have become increasingly important for electronic devices requiring large voltage and current control. The development of power electronics technology has had a significant impact, especially in AC motor drives, power control units and industrial applications. In recent years, DC-DC converters have played an important role in terms of energy efficiency, reliability and sustainability, especially in renewable energy sources (Mumtaz et al., 2021). CUK converters, which consist of two inductors and two capacitances, are a type of fourth-order DC-DC converter. CUK converters are circuit topologies that transfer the DC voltage level applied to the input to a higher or lower level to the output by appropriate control methods (Narayanaswamy and Mandava, 2023). CUK converters have an output voltage in the opposite polarity of the input voltage (Singh, 2017).

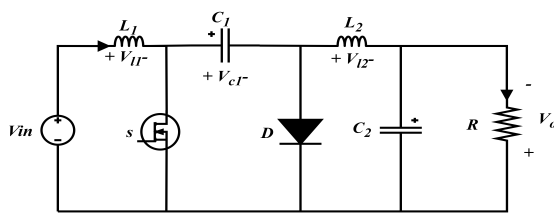


Figure 1: Cuk converter topology.

CUK converters are obtained by cascading the Boost converter and Buck converter topologies. For this reason, they have the ability to both increase and decrease the input voltage. The most important advantage of these converters is the presence of inductance at the input and output of the circuit. In this way, current fluctuations are reduced to a minimum level. The visual of the CUK converter topology is presented in Figure 1.

The CUK converter topology operates in two operating modes, Pulse Width Modulation (PWM) rising edge and falling edge triggering. When the MOSFET is triggered by the rising edge, the inductance L_1 is energized by the source voltage V_{in} and the energy is stored as a magnetic field. Capacitor C_2 is discharged to ground through the MOSFET and energizes inductor L_2 and the load, the diode exhibits open circuit characteristics. The electrical equivalent circuit of the CUK converter MOSFET on mode is shown in Figure 2. The mathematical equations for this case are given in Equation (1) (Yilmaz et al., 2020).

$$\left. \begin{aligned} \frac{di_{L_1}}{dt} &= \frac{1}{L_1} (V_{in} - V_{c_1}) \\ \frac{dV_{c_1}}{dt} &= \frac{1}{C_1} i_{L_1} \\ \frac{di_{L_2}}{dt} &= \frac{1}{L_2} (-V_0) \\ \frac{dV_0}{dt} &= \frac{1}{C_2} \left(i_{L_2} - \frac{V_0}{R} \right) \end{aligned} \right\} \quad (1)$$

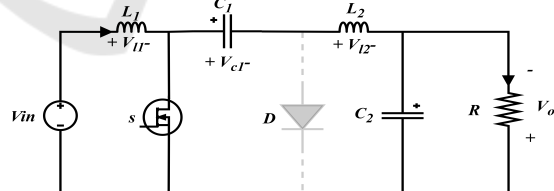


Figure 2: Switching element conduction state CUK converter circuit topology.

When the MOSFET low pulse is triggered, the energy stored in inductor L_1 is transferred to capacitor C_1 and indirectly in inductor L_2 . The diode is in on mode for this situation. Energy is supplied to the load through inductor L_2 . The electrical equivalent circuit of the CUK converter MOSFET cut-off mode is shown in Figure 3. The mathematical equations for this case are given in Equation (2) (Yilmaz et al., 2020).

$$\left. \begin{aligned} \frac{di_{L_1}}{dt} &= \frac{1}{L_1} (V_{in} - V_{c_1}) \\ \frac{dV_{c_1}}{dt} &= \frac{1}{C_1} i_{L_1} \\ \frac{di_{L_2}}{dt} &= \frac{1}{L_2} (-V_0) \\ \frac{dV_0}{dt} &= \frac{1}{C_2} \left(i_{L_2} - \frac{V_0}{R} \right) \end{aligned} \right\} \quad (2)$$

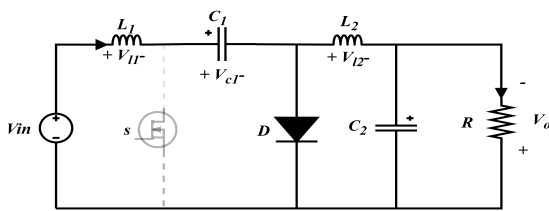


Figure 3: Switching element cut-off status CUK converter circuit topology.

Table 1 gives the mathematical expressions of the electrical circuit parameters of the CUK converter topology used in the study.

Table 1: Mathematical expressions of electrical circuit parameters of CUK converter topology.

Parameter	Formula
Duty Cycle	$D = \frac{ V_{in} }{V_S + V_{in} }$
Inductance	$L_1 = \frac{DV_S}{\Delta i_{L_1} f_S}$ $L_2 = \frac{DV_S}{\Delta i_{L_2} f_S}$
Capacitance	$C_1 = \frac{DV_{in}}{\Delta V_{C_1} R f_S}$ $C_2 = \frac{D - 1}{8} \frac{\Delta V_{in}}{V_{in} f_S^2}$
Load	R
Switching Frequency	f_S

2.2 High Order Sliding Mode Control

Higher order sliding mode control (HOSMC) is a control method developed from Sliding Mode Control (SMC). It is used to provide simplicity, high performance, stability and vibration reduction to nonlinear systems. HOSMC includes tracking calculation, shift calculation and supertwist calculation. Its advantages over sliding mode controllers are that it is more robust against the uncertain behaviour of the system and provides faster response and provides superior perfor-

mance by preventing the system from vibration. The mathematical expressions used for HOSMC are given in Equations 3-6 (Yilmaz and Corapsiz, 2025).

$$u_1(t) = \lambda_1 \sqrt{|S|} \operatorname{sign}(S) \quad (3)$$

$$u_2(t) = \lambda_2 \int \operatorname{sign}(S) dt \quad (4)$$

$$u_3(t) = \lambda_3 \operatorname{sign}(S) \quad (5)$$

$$u(t) = \lambda_1 \sqrt{|S|} \operatorname{sign}(S) + \lambda_2 \int \operatorname{sign}(S) dt + \lambda_3 \operatorname{sign}(S) \quad (6)$$

In Equation 3, it pulls the system quickly to the sliding surface. It provides terminal attraction behaviour. In Equation 4, it is added so that the system does not make permanent errors. It is known as integral sliding mode control and is more resistant to disturbances. In Equation 5, it pulls the system quickly to the sliding surface but can cause unwanted vibrations called flutter. In Equations 3-6, λ_1 , λ_2 , λ_3 the coefficients that provide the balance between convergence speed, steady-state accuracy, and jitter reduction.

3 RESULTS AND DISCUSSION

In this study, the dynamic performance of the CUK converter is evaluated using HOSMC and PI controller. The dynamic performance of the CUK converter is evaluated in detail for four different scenarios. Considering the increase/decrease of the output voltage, important performance criteria such as efficiency and settling time are analysed.

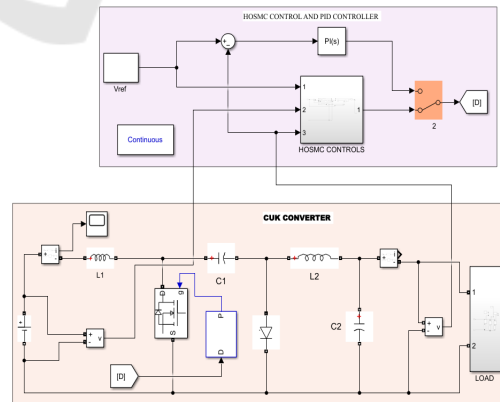


Figure 4: Simulation model of the CUK converter with PI control and HOSMC.

The parameters of the CUK converter used in the simulation studies are; capacitors $C_1 = 12.35 \mu F$, $C_2 = 10.42 \mu F$, inductors $L_1 = 800 \mu H$

ve $L_2 = 1600 \mu H$ and load $R = 36 \Omega$. The output voltage of the CUK converter is -60V in the first scenario, and -45V, -15V in the third scenario, first in the fourth scenario 1.5 per second -60V and next 1.5 per second -45V. Figure 4 shows the CUK converter designed in MATLAB/SIMULINK 2021b to evaluate the performance of the controllers under different scenarios. The input voltage for all scenarios is 30V was taken as fixed.

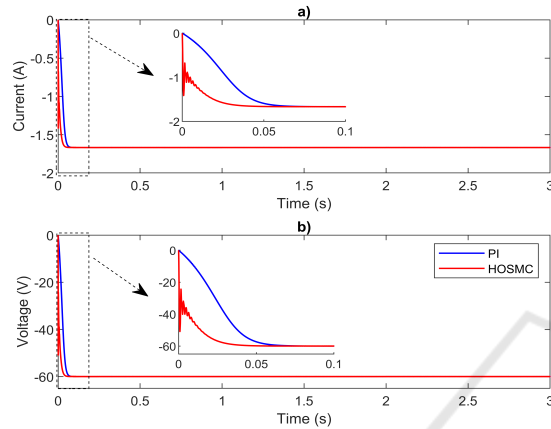


Figure 5: Load a) current-time b) voltage-time changes for the first scenario.

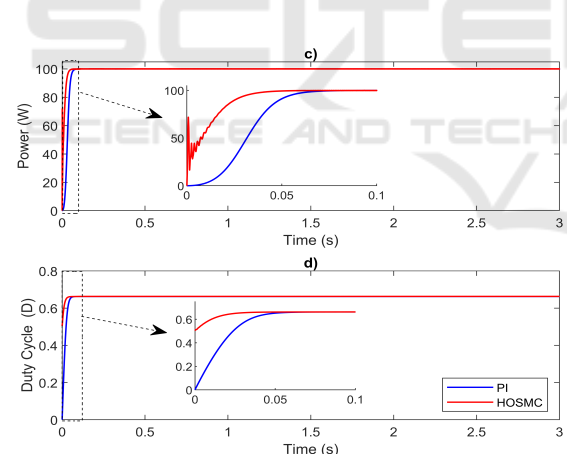


Figure 6: Load a) power-time b) duty cycle-time variations for the first scenario.

In the first scenario, the input voltage is reverse polarity. 60 VDC voltage. In this scenario, the PI controller and HOSMC's ability to increase the input voltage by two times was evaluated. According to the HOSMC PI controller, the duty cycles 0.04. It was observed that the output voltage reached its steady state by finding the best value in seconds. 0.01% tolerant -60 DC nominal voltage is fixed, and energy conversion efficiency is measured as 100%. Figure 5 shows the changes in load current and voltage with respect to

time. Figure 6 shows the changes in power and duty cycle with respect to time.

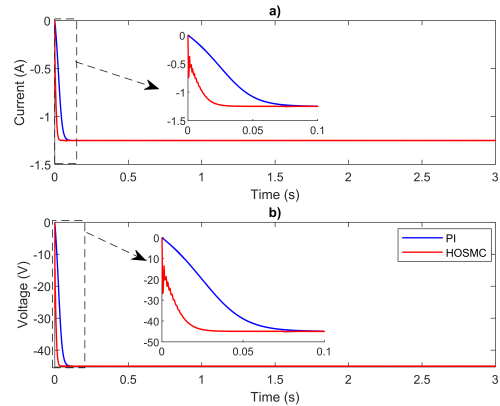


Figure 7: Load a) current-time b) voltage-time changes for the second scenario.

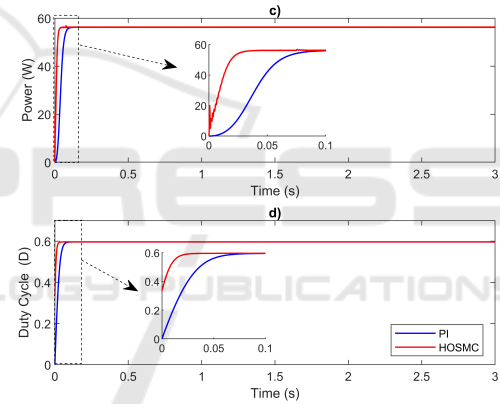


Figure 8: Load a) power-time b) duty cycle-time variations for the second scenario.

In the second scenario, the voltage boost performance of the controllers 30 V. In this scenario, the system's transient behavior and steady-state performance were observed. According to the PI controller, the most optimum value of the HOSMC duty cycle was 0.03 seconds and reached its steady state. Output voltage %0,01 tolerant -45VDC voltage value was reached and energy conversion efficiency was obtained as 100%. The changes of load current and voltage with respect to time are given in Figure 7. The changes of power and duty cycle with respect to time are shown in Figure 8.

In the third scenario, the performance of HOSMC and PI controllers in reducing the input voltage level by half is examined. While HOSMC reaches the most optimum value of the duty cycle in 0.05 seconds, PI controller reaches the most optimum value of the duty

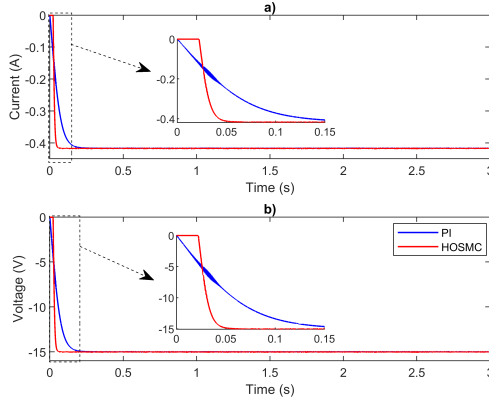


Figure 9: Load a) current-time b) voltage-time changes for the third scenario.

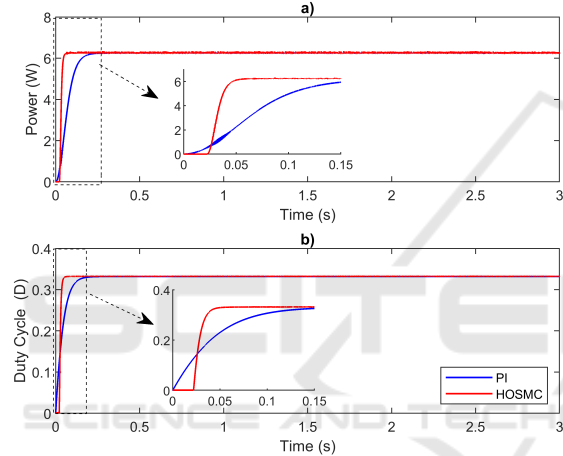


Figure 10: Load a) current-time b) voltage-time changes for the third scenario.

cycle in 0.15 seconds. HOSMC control structure not only reaches the optimum duty cycle in a shorter time to ensure the stability of the system, but also exhibits superior performance in transient behaviors. In particular, the fact that the duty cycle becomes stable in only 0.05 seconds reveals the fast response ability of the system. The changes in the load current and voltage values with respect to time are given in Figure 9, and the changes in the power and duty cycle with respect to time are given in Figure 10.

In the fourth scenario, the performances of the PI controller and HOSMC were evaluated for different voltage levels in different time periods. The input voltage was increased from 30V to 60V for the first 1.5 seconds. The voltage value of 60V was decreased to 45V for the next 1.5 seconds. For this scenario, it was observed that the HOSMC had a shorter settling time compared to the PI controller in the first 1.5 seconds. The results of this scenario are shown in Figure 11 and Figure 12.

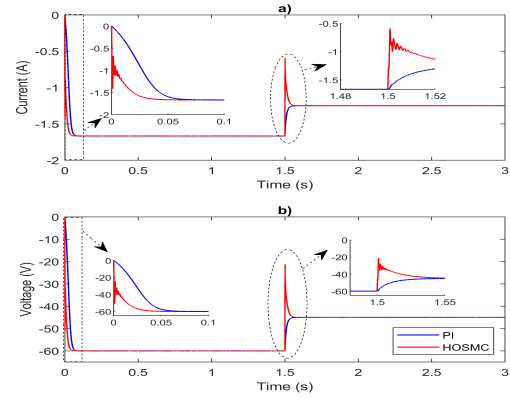


Figure 11: Load a) current-time b) voltage-time changes for the second scenario.

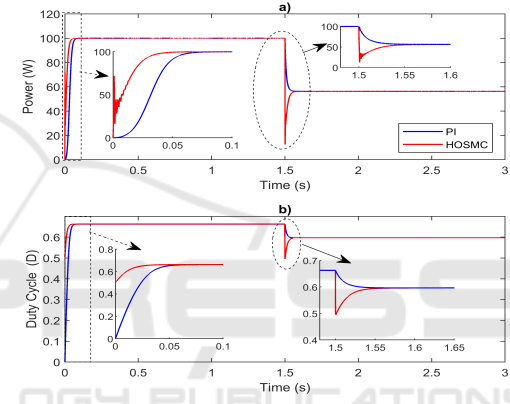


Figure 12: Load a) power-time b) duty cycle-time variations for the second scenario.

4 CONCLUSIONS

In this study, the dynamic behavior of PI controller and HOSMC in CUK converter is comparatively analyzed in terms of current, voltage, power and duty cycle. Four different scenarios are evaluated in the study. In all scenarios, HOSMC exhibits shorter convergence time capability compared to PI controller. In the first two scenarios, the voltage boost feature of CUK converter is evaluated, and in the third scenario, the voltage reduction feature. In the fourth scenario, the desired output voltage sudden change is evaluated. In all scenarios, HOSMC and PI controller reach 100% efficiency. HOSMC exhibits strong resistance by behaving more robustly against uncertainties and external disturbances in the system. In addition, it has the advantages of faster transient response, lower overshoot and shorter settling time thanks to its high-order derivative feedback structure. HOSMC's discrete-time operating structure and high accuracy

enable it to provide superior control performance especially in nonlinear and parameter-variable systems. With these aspects, HOSMC gave more successful results than the PI controller in terms of both control quality and system reliability

ACKNOWLEDGEMENTS

This work was supported by the Ataturk University Coordination Unit of Scientific Research Projects (Project No: FBA-2025-15043)

REFERENCES

Balestrino, A., Landi, A., and Sani, L. (2002). Cuk converter global control via fuzzy logic and scaling factors. *IEEE Transactions on Industry Applications*, 38(2):406–413.

Chen, Z. (2012). Pi and sliding mode control of a cuk converter. *IEEE Transactions on Power Electronics*, 27(8):3695–3703.

Fathabadi, H. (2016). Novel high efficiency dc/dc boost converter for using in photovoltaic systems. *Solar Energy*, 125:22–31.

Ilman, S. M., Dahono, A., Prihambodo, M. A. K., Putra, B. A. Y., Rizqiawan, A., and Dahono, P. A. (2019). Analysis and control of modified dc-dc cuk converter. In *Proc. 2nd Int. Conf. High Voltage Engineering and Power Systems (ICHVEPS)*.

Mahho, M., Yilmaz, M., and Çorapsız, M. F. (2025). The performance of modified sepic converter for dynamic conditions with pi controller. In *2025 7th International Congress on Human-Computer Interaction, Optimization and Robotic Applications (ICHORA)*, pages 1–4.

Mumtaz, F., Yahaya, N. Z., Meraj, S. T., Singh, B., Kannan, R., and Ibrahim, O. (2021). Review on non-isolated dc-dc converters and their control techniques for renewable energy applications. *Ain Shams Engineering Journal*, 12(4):3747–3763.

Narayanaswamy, J. and Mandava, S. (2023). Non-isolated multiport converter for renewable energy sources: A comprehensive review. *Energies*, 16(4):1834.

Refaat, A., Elbaz, A., Khalifa, A.-E., Elsakka, M. M., Kalas, A., and Elfar, M. H. (2024). Performance evaluation of a novel self-tuning particle swarm optimization algorithm-based maximum power point tracker for proton exchange membrane fuel cells under different operating conditions. *Energy Conversion and Management*, 301:118014.

Singh, S. (2017). Selection of non-isolated dc-dc converters for solar photovoltaic system. *Renewable and Sustainable Energy Reviews*, 76:1230–1247.

Xu, L., Guerrero, J. M., Lashab, A., Wei, B., Bazmohammadi, N., Vasquez, J. C., and Abusorrah, A. (2021). A review of dc shipboard microgrids—part i: Power architectures, energy storage, and power converters. *IEEE Transactions on Power Electronics*, 37(5):5155–5172.

Yilmaz, M., Corapsiz, M., and Çorapsız, M. R. (2020). Voltage control of cuk converter with pi and fuzzy logic controller in continuous current mode. *Balkan Journal of Electrical and Computer Engineering*, 8(2):127–134.

Yilmaz, M. and Çorapsız, M. F. (2025). A robust mppt method based on optimizable gaussian process regression and high order sliding mode control for solar systems under partial shading conditions. *Renewable Energy*, 239:122339.

Yilmaz, M., Çorapsız, M. R., and Çorapsız, M. F. (2025). A novel maximum power point tracking approach based on fuzzy logic control and optimizable gaussian process regression for solar systems under complex environment conditions. *Engineering Applications of Artificial Intelligence*, 141:109780.